Phase-Responsive Fourier Nanotransducers for Probing 2D Materials and Functional Interfaces

DOI:
10.1002/adfm.201902692

Document Version
Accepted author manuscript

WILEY-VCH

Article type: Communication

Phase-responsive Fourier nanotransducers for probing 2D materials and functional interfaces

Andrei V. Kabashin, Vasyl G. Kravets, Fan Wu, Shinji Imaizumi, Victoria O. Shipunova, Sergey M. Deyev, Alexander N. Grigorenko**

Prof. A. V. Kabashin
Aix Marseille Univ, CNRS, LP3, Marseille, France
E-mail: kabashin@lp3.univ-mrs.fr
Dr. V. G. Kravets, Dr. Fan Wu, Prof. A. N. Grigorenko
School of Physics and Astronomy, University of Manchester, Manchester, M13 9PL, UK
E-mail: sasha@manchester.ac.uk
Prof. A. V. Kabashin, Dr. V. O. Shipunova, Prof. S. M. Deyev
MEPhI, Institute of Engineering Physics for Biomedicine (PhysBio), 115409 Moscow, Russia
Dr. V. O. Shipunova, Prof. S. M. Deyev
Shemyakin–Ovchinnikov Institute of Bioorganic Chemistry, Russian Academy of Sciences, 16/10 Miklukho-Maklaya St, Moscow 117997, Russia
Dr. Fan Wu
Key Laboratory for Non-Equilibrium Synthesis and Modulation of Condensed Matter (Ministry of Education), School of Science, Xi'an Jiaotong University, Xi'an, Shaanxi 710049, China
Dr. S. Imaizumi, Novel Functional Materials Research Laboratory Advanced Technology Research Division SONY Corporation, Japan

Keywords: Fourier nanotransducers, plasmonic metamaterials for biosensing, 2D materials, plasmonic biosensors, label-free biosensing

Abstract.

Light scattered by an object contains plethora information about the object which is distributed evenly among all possible Fourier components of light observed in the far-field. There are some cases, however, where this information is accumulated in the light confined by the object and then encoded in just a few coherent optical beams. Here, Fourier nanotransducers based on 2D plasmonic metamaterials are introduced, which are capable of confining light in 2D plane contacting with a functional interface, gathering information about its properties and then transmitting the information into discrete optical beams with amplified phase relations. It is shown that phase of light in such beams can be used for probing dynamic physical properties of 2D materials and performing bio/chemical sensing with unprecedented sensitivity. Using a

Fourier transducer based on periodic gold nanostructures, ferroelectric response from a single atomic layer of MoS_2 is resolved and studied for the first time, as well as the detection of important antibiotic chloramphenicol at fg/mL level is demonstrated, which several orders of magnitude better than reported in the literature. The implementation of phase-responsive Fourier nanotransducers opens new avenues in exploration of emergent 2D structures and radical improvement of biosensing technology.

Capable of exhibiting properties not found in nature, artificial nanostructured materials offer unique opportunities to concentrate light and manipulate its characteristics.[1-4] For example, phase of light can be effectively manipulated by 2D nanostructured metasurfaces providing new laws of reflection and refraction as well as designer beam shapers.[5,6] Systematic studies of light phase changes in space domain have a long successful history and resulted in several breakthrough technologies, such as holography[7] and phase contrast.[8] Changes of light phase under evolution of a nanomaterial with time attracted significantly less attention. This seems to be surprising as behaviour of light phase in time domain was paramount for detection of faint signals associated with gravitational waves[9] and important for development of compact and fast phase light modulators[10] among others important advancements.

Nanotransducers enabling manipulations of light phase in 2D plane are of particular importance as they could provide breakthrough tools for studying properties of planar structures and functional interfaces, including newly emerging 2D materials and van der Waals heterostructures[11] that promise appealing applications in electronics, optics, photochemistry, biomedicine, etc. The optical response of 2D materials was extensively used for elucidating their physical properties; however, currently available methods (absorption spectroscopy, Raman, photoluminescence) provide mostly basic information and normally cannot gather

dynamic characteristics due to difficulty of signal collection from atomically thin layers. The involvement of light phase properties can offer an additional sensitive parameter to characterize 2D materials, as it was already demonstrated in investigations of ferromagnetic properties of van der Waals heterostructures (down to monolayer) using phase detection in simple (unamplified) regime.[12,13] Dynamic control of 2D functional interfaces presents another important application for phase-sensitive transducers. Optical biosensing is a prominent example as it implies time monitoring of refractive index changes in ultrathin (less than a few nm) biological layers due to biomolecular binding events between a target analyte coming from a solution and its corresponding receptor immobilized on the surface.[14] As shown in previous studies, light phase can be orders of magnitude more sensitive to environment as compared to light amplitude in tasks of plasmonic biosensing when biological events are probed on plasmon-supporting gold films[15] or designed nanoarrays.[16,17]

Here we introduce metastructures based on Fourier nanotransducers for ultrasensitive characterization of properties of 2D materials and functional interfaces, which are designed to confine light in the plane of studied 2D object and thus sensitively accumulate information about its properties and encode the information into discrete optical beams with amplified phase relations to enable unlimited raw phase sensitivity to temporal variations in the examined object. To demonstrate potential of Fourier nanotransducer metamaterials, we for the first time observe ferroelectric behavior in a single atomic layer of MoS_2 and demonstrate detection limit of fg/mL concentration of chloramphenicol, a critically important antibiotic used in medicine and food industry, which is at least three orders of magnitude better than previously achieved with all label-free or label-counterparts.

To explain the main idea, let us consider a general case of light scattering by an illuminated examined object. If a studied object is periodically ordered, then, light interference

affects the far-field domain and the scattered light can be written[18] as a discrete sum of Fourier components $\mathbf{E}_{sc}(\mathbf{r},t)=\sum_n E_n\hat{\boldsymbol{\varepsilon}}_n \exp(i\mathbf{k}_n\mathbf{r}-i\omega t)$, where index *n* incorporate both the beam number and the light polarization and $E_n=|E_n|\exp(\iota\Delta_n)$ is the complex amplitude of discrete Fourier component. We will refer to such materials as discrete Fourier materials (DFM). DFMs allow one interrogate not only the amplitude of the scattered light in the far-field but also its phase. Figure 1a shows a typical example of light scattering by DFM-based transducer designed for studies of properties of 2D materials.

The phase Fourier nanotransducers (PFN) are then defined as discrete Fourier materials, which make possible concentration of light in 2D plane and thus enable abrupt dependence of the phase of the beam orders on properties of an adjacent 2D medium. This provides responsive temporal control of light phase induced by tiny variations of the 2D medium. The amplitude and the phase of the *n*-th beam (Figure 1a) contain all relevant information about the studied sample. This information, however, is not specific and to improve selectivity, one normally has to measure spectral and angular dependence of reflection using, e.g., variable angle spectroscopic ellipsometry.[19] We then postulate that phase of light produced by PFNs becomes an efficient parameter for characterization of 2D materials and interfaces if two conditions are satisfied: (i) PFNs exhibit a sudden change of light beams in the discrete orders at the measurement conditions. For example, a loss of intensity in reflection is always accompanied by enhanced phase sensitivity[15,20]. (ii) Probing light of PFN is confined in the plane of 2D material conditioning ultrasensitive phase response on variation of its properties.

Figure 1 (b-d) describes three methods for the implementation of PFN, which could unlock ultra-high phase response from 2D structures. First method is based on darkness where the phase of the light is changing in an abrupt fashion and the light is concentrated in 2D plane, see Figure 1b. (Previously described thin films and metamaterials enabling light darkness [15-17]

could also be suitable provided they concentrate the light in 2D plane.) We showed that the increase of phase sensitivity over amplitude one, *G*, can be described by a simple relation $G \sim 1/\Psi_{\min}$, where $\Psi_{\min} \approx E_n / E_0$, for details see Ref. 16. The second method of creating PFNs is based on disappearance of the diffraction orders, Figure 1c. Indeed, the number of orders in DFM is not fixed and can change when the properties of a studied medium is changed. This would lead to a rearrangement of all beams produced by scattering and extremely fast changes of phase and amplitude of light in all orders. The most famous example of this case is Rayleigh cut-off phenomenon where a diffraction order disappears (or appears) for a sample fabricated on a substrate with refractive index different from that of the measured medium[21]. Finally, Figure 1d shows the third method of creating PFN, which is based on guided modes of light. This case does not require rearrangement of diffraction orders. Instead, a periodic arrangement of metamaterial elements produces optical beams channelled along the nanomaterials elements. As a result, these elements strongly modulate the phase of the channelled beam providing extremely high phase sensitivity to tiny changes of the medium surrounding nanomaterials.

The enhancement of phase sensitivity achieved with PFNs over the standard optical interrogation can be approximated by the following relation $G \sim \frac{E_{loc}}{E_n}\frac{L_{prop}}{\lambda}$, where E_{loc} is the local field acting on 2D material or interface, E_n is the light field amplitude in *n*-th Fourier component, L_{prop} is the characteristic propagation length of the trapped mode and λ is the light wavelength. Since E_n can be made arbitrary small, it implies that the raw phase sensitivity of PFNs has no limits.

In this work, we show two generic applications of PFNs for studying physical properties of 2D materials and label-free biosensing based on functional interfaces. First, we describe

investigation of ferroelectricity in a single layer of molybdenum disulphide with the help of PFNs. The most common (stable) 1H phase of a single layer MoS_2 does not possess ferroelectric properties due to its symmetry.[22] The chemical vapor processes can induce the transition of 1H phase of MoS_2 to a metastable 1T phase with lower symmetry.[23] 1T phase of MoS_2 is metallic and could be relatively stable (it is relaxed back to a semiconductor 1H state by annealing in vacuum at 400°C). Its symmetry allows piezoelectric behaviour while ferroelectric behaviour is still forbidden.[22] In the presence of substrate (pressure, adsorbates), 1T phase becomes unstable and subject to Peierls-like instability which leads to the formation of semiconductor 1T′ phase of MoS_2.[24] (It was also suggested that hydrogen adsorbates can even stabilize 1T′ phase over 1H one.[24]) The symmetries of 1T′ phase of MoS_2 allows ferroelectricity (perpendicular to the plane) which was indeed predicted to exist at room temperature in this polytype of MoS_2[25] but is yet to be observed.

To measure the ferroelectric response of a single layer MoS_2 we have chosen PFNs which incorporates darkness and guiding modes. The schematic of the waveguide/plasmonics array hybrid PFN structure is shown in Figure 2a. It includes a gold sublayer (65 nm) deposited on a glass substrate with a periodic gold grating (period 1560 nm, thickness 70 nm, the stripe width 475 nm) fabricated on the top of gold film and covered with 300 nm of Si_3N_4. The hybrid optical modes of this structure were earlier discussed[26]. A CVD grown single layer MoS_2 (supplied by 2D Semiconductors) was transferred on the top of the structure, Figure 2a, with the help of the wet transfer procedure. Figures 2b and 2c show the optical and SEM images of the studied sample, respectively. To identify regions with a high concentration of 1T/1T′ phases in a transferred MoS_2 we apply Raman spectroscopy. 1T/1T′ phases possess a set of J_1, J_2 and J_3 Raman frequencies[27,28] lying in the range of 150-350 cm^{-1}. Figure 2d shows a typical Raman spectrum from a region with high concentration of 1T/1T′ phase of MoS_2 with the marked

Raman peaks J_1, J_2 and J_3. To verify the prevalence of semiconductor 1T′ phase over metallic 1T phase in these regions, we measured the 2D analogue of the Franz-Keldysh effect[29] in the sample reflection near the predicted bandgap of 0.7 eV of the 1T′ phase.[25] Figure 2e shows a relatively strong change of reflection of the structure (measured at normal light incidence using Fourier Transform Infra-Red spectrometer) with applied gating voltage at the wavelengths just below the bandgap (voltage was applied between gold nanostructure and a MoS_2 single layer) which suggests that we indeed have the presence of 1T′ phase in the studied region of a MoS_2 flake. The spectrum of ellipsometric reflection of the structure at an incident angle of 80° is depicted at Figure 2f. (It is plotted in ellipsometric parametres Ψ and Δ such that $r_p / r_s = \tan(\Psi)\exp(i\Delta)$, where r_p and r_s are complex amplitude reflection coefficients for *p*- and *s*-polarization, respectively[19]). There are two points in the spectrum with amplified phase relations: one corresponding to $r_p = 0$ at wavelength ~540nm and another one corresponding to r_s=0 at 624 nm. For studying ferroelectric behaviour of MoS_2, we have chosen the singular point in *s*-reflection (at 624 nm) as in-plane electric fields of light are more sensitive to the charges induced on MoS_2 by gating. Figure 2g shows the main result of our measurements – hysteretic behaviour of measured light phase as a function of gating voltage. (The hysteresis was absent in the amplitude interrogation and in regions of MoS_2 without pronounced Raman peaks J_1, J_2 and J_3). The switching voltage is around $V_{sw} \approx 100$ V and corresponds to switching fields of $E = V_{sw} / d_{Si_3N_4} = 3 \cdot 10^6$ V/cm which is the same order of magnitude as the predicted value of 10^7 V/cm.[25] It is difficult to evaluate the spontaneous polarization, p_z, from our data as the change of the phase Δ can be also induced by the change of the electron density in MoS_2. The induced electron density at the 100 V was $n = \dfrac{\varepsilon_{Si_3N_4} V}{4\pi d_{Si_3N_4}} = 1.5 \cdot 10^{13}$ cm^{-2} and corresponded

to the phase change of $\Delta\varphi_0 \approx 1.5°$. A crude top limit for p_z can be estimated from the open hysteresis of $\Delta\varphi_h \approx 0.14°$ as $p_z = \frac{\Delta\varphi_h}{\Delta\varphi_0} ne = 0.22\,\mu$ C/cm^2. This value is quite close to the predicted value of $p_z = 0.2$ μC/cm^2 for 1T′ phase of molybdenum disulphide.[25]

For investigation of functional interfaces, we fabricated 2D nanotransducers which incorporate darkness, grazing beams and disappearance of diffraction orders in attenuated total reflection geometry. Simultaneous generation of these three phenomena becomes possible due to diffraction coupling of localized plasmon resonances over periodically arranged individual metamaterial elements (nanodots, nanostripes, etc.).[4,16,17] A scheme of such PFNs for examining 2D interfaces is shown in Figure 3a. One can see that the reflected beam shows the darkness at the wavelength of ~600nm realized due to diffraction coupling of localized plasmon resonances[4]. At the same time, the diffracted beam becomes really strong at the condition of Rayleigh anomaly[21] and disappears completely when the diffraction order moves into the substrate concentrating at the plane of the examined 2D object. The left inset in Figure 3a shows a well-defined spectral spike at the wavelength of the reflection darkness measured for grazing beam geometry, which confirms the generation of a planar mode at the diffraction edge conditions. Figure 3b depicts SEM 3D image of the nano-antenna metamaterial sample used in this work while Figure 3c shows the ellipsometric reflection at the resonance conditions when the structure shown in Figure 3b contacts aqueous ambience.

We apply the PFNs shown in Figure 3 for label-free biosensing. To this end, we developed a novel protocol for a quantification of chloramphenicol (CAP, D(-)-threo-2-dichloroacetamido-1-*p*-nitro-phenyl-1,3-propanediol), a critically important small molecular weight (323 Da) antibiotic against gram-positive and gram-negative bacteria, which is widely used in clinical and veterinary applications. Since a regular consumption of CAP with food and

other products may lead to serious adverse effects for human health (leukemia, aplastic anemia and cardiovascular collapse), precise and sensitive quantification of CAP is critically important. A schematic description of functionalization steps on nanoparticle surface to implement the CAP detection protocol is illustrated in Figure 4a.

The quantification of CAP was realized in a label-free competitive assay mode (see short and detailed descriptions in Figure 4b and in Supplementary Information, respectively). The detection was carried out in phosphate-buffered solution, pH 7.4 supplemented with 1% of bovine serum albumin since it is frequently used buffer similar to physiological conditions. As shown in Figure 4c, the change of CAP concentration in the pumped solutions from 10^6 ng/mL to 0 ng/mL leads to a gradual spectral shift of the resonance position until it comes to saturation at the concentration of 10^{-3} ng/mL. The limit of detection (LOD) for minimal CAP concentration based on spectral data was determined by 3σ criterion and found to be 25 pg/mL (Supplementary Information), which is already better than LOD values from all previous studies for label-free methods (e.g., LOD equal to 0.26 ng/mL,[30] 32.2 pg/ml,[31] 30 pg/mL[32]) and not far from best values for label-based methods such as EIA assays (7.6 ng/mL,[33] 6 pg/mL[34]).

It is the phase interrogation, however, which is expected to provide hypersensitivity. As shown in Figure 4c, phase started to evolve only after the third concentration of CAP, which was obviously related to the beginning of fast variation range within its singularity (Figure 3c). Then, using phase as a signal parameter we could follow all subsequent concentrations of CAP, while the whole phase variation nearly reached its full dynamic range (180 deg). Finally, phase started to come to saturation at last points, which is consistent with complete binding of all active CAP sites on Au nanoparticles by the antibodies. The error of phase measurements provided by the ellipsometer for a fixed angle of incidence and the spectral operation range of

600-800 nm is 0.05 deg. Using this value of the error, we can estimate the relevant LOD as 27 fg/mL, which is almost 3 orders of magnitude better than all values recorded by alternative techniques. As we reported in our previous study[15], a much better phase resolution of 10^{-3} deg. (and lower) can be obtained, e.g., by using advanced phase sensitive systems based on low-noisy acousto-optical modulators. It is easy to find that with such a phase resolution the LOD can be below 1 fg/mL, i.e. in the sub-fg/mL level. It is important that this spectacular result can be obtained in the absence of the labelling step, which requires extra time and cost demands, as well as often occludes the binding site provoking false negative signals[14]. Furthermore, the used optical arrangement enables one to follow biomolecular interactions in real time and thus obtain additional information on kinetic constants of reactions, which is hardly possible with labelling approaches.

To conclude, advanced materials based on Fourier nanotransducers provide wherewithal to study dynamic properties of 2D materials and functional interfaces with unprecedented sensitivity. In particular, using PFN light phase response we observe ferroelectric behavior of 1T′ phase of single layer MoS_2, recently predicted by theory. We envisage a wide application of PFNs for studying ferroelectricity in other 2D materials. We showed that PFN can help to exceed LODs of current state-of-the-art label-free[30-32] and label-based[33,34] biosensors by 4 and 3 orders of magnitude, respectively. We believe that such hypersensitivity can radically advance label-free biosensing technology and eventually extend its application area beyond research laboratories. Here, we envision several biomedical, safety and security tasks, which could profit from the reported hypersensitivity. These include the detection of deadly pathogens to timely diagnose the progression of deadly diseases in clinical applications[35] and the detection of ultra-small concentrations of drugs in sports doping.[36] We also see the detection of highly toxic biotoxins for environmental safety and counter-bioterrorism applications.[37]

Finally, PFNs can be applied for monitoring of pathogens, drugs and other components in food samples. The detection of some target analytes in complex matrices (meet, honey, milk etc.) presents a real challenge due to high viscosity of these products, which requires complicated treatment procedures to separate all matrix components.[38] The increase of sensitivity makes possible 1000-time dilution of samples and their direct and prompt analysis. Finally, PFNs can find their applications in other time domain control of light phase, e.g., compact light modulators and light multiplexers.

Supporting Information

Supporting Information is available from the Wiley Online Library or from the author.

Acknowledgements

ANG acknowledges the support from the European Union's Horizon 2020 research and innovation programme under grant agreement No. 696656 GrapheneCore1/GrapheneCore2 and SONY research grant agreement. AVK acknowledges the support from Excellence Initiative of Aix-Marseille Univ - A*MIDEX, a French "Investissements d'Avenir" program, ITMO "Plan Cancer 2014–2019" INSERM program and MEPhI Academic Excellence Project (Contract No. 02.a03.21.0005).

Received: ((will be filled in by the editorial staff))
Revised: ((will be filled in by the editorial staff))
Published online: ((will be filled in by the editorial staff))

[1] Y. Liu, X. Zhang, *Chem. Soc. Rev*., **2011**, 40, 2494.

[2] A. N. Grigorenko, A. K. Geim, H. F. Gleeson, Y. Zhang, A. A. Firsov, I. Y. Khrushchev, J. Petrovic, *Nature* **2005**, *438*, 335.

[3] B. Luk'yanchuk, N. I. Zheludev, S. A. Maier, N. J. Halas, P. Nordlander, H. Giessen, C. T. Chong, *Nat. Mater.* **2010**, *9*, 707.

[4] V. G. Kravets, A. V. Kabashin, W. L. Barnes, A. N. Grigorenko, *Chem. Rev.*, **2018**, *118*, 5912.

[5] N. Yu, P. Genevet, M. A. Kats, F. Aieta, J.-P. Tetienne, F. Capasso, Z. Gaburro, *Science*, **2011**, *334*, 333.

[6] A. V. Kildishev, A. Boltasseva, V. M. Shalaev, *Science*, **2013**, *339*, 1232009.

[7] D. A. Gabor, *Nature*, **1948**, *161*, 777.

[8] F. Zernike, *Science,* **1955**, *121*, 345.

[9] B. P. Abbott et al, *Phys. Rev. Lett.,* **2016***, 116,* 061102.

[10] A. Melikyan, L. Alloatti, A. Muslija, D. Hillerkuss, P. C. Schindler, J. Li, R. Palmer, D. Korn, S. Muehlbrandt, D. Van Thourhout, B. Chen, R. Dinu, M. Sommer, C. Koos, M. Kohl, W. Freude, J. Leuthold, *Nat. Photon*., **2014**, *8*, 229.

[11] A. K. Geim, I. V. Grigorieva, *Nature*, **2013**, *499*, 419.

[12] C. Gong, L. Li, Z. Li, H. Ji, A. Stern, Y. Xia, T. Cao, W. Bao, C. Wang, Y. Wang, Z. Q. Qiu, R. J. Cava, S. G. Louie, J. Xia, X. Zhang, *Nature*, **2017**, *546*, 265.

[13] B. Huang, G. Clark, E. Navarro-Moratalla, D. R. Klein, R. Cheng, K. L. Seyler, D. Zhong, E. Schmidgall, M. A. McGuire, D. H. Cobden, W. Yao, D. Xiao, P. Jarillo-Herrero, X. Xu, *Nature*, **2017**, *546*, 270.

[14] B. Huang, G. Clark, E. Navarro-Moratalla, D. R. Klein, R. Cheng, K. L. Seyler, D. Zhong, E. Schmidgall, M. A. McGuire, D. H. Cobden, W. Yao, D. Xiao, P. Jarillo-Herrero, X. Xu, *Nature*, **2017**, *546*, 270.

[15] A. V. Kabashin, S. Patskovsky, A. N. Grigorenko, *Opt. Exp.*, **2009**, *17*, 21191.

[16] V. G. Kravets, F. Schedin, A. V. Kabashin, A. N. Grigorenko, *Opt. Lett.*, **2010**, *35*, 956.

[17] V. G. Kravets, F. Schedin, R. Jalil, L. Britnell, R. V. Gorbachev, D. Ansell, B. Thackray, K. S. Novoselov, A. K. Geim, A. V. Kabashin & A. N. Grigorenko, *Nat. Mater.*, **2013**, *12*, 304.

[18] M. Born, E. Wolf, *Principles of Optics*, Cambridge University Press, **1980**.

[19] R. M. A. Azzam, N. M. Bashara, *Ellipsometry and Polarized Light*, North-Holland, **1977**.

[20] A. N. Grigorenko, P. I. Nikitin, A. V. Kabashin, *Appl. Phys. Lett.*, **1999**, *75*, 3917.

[21] A. Hessel, A. A. Oliner, *Appl. Opt.*, **1965**, *4*, 1275.

[22] C. Cui, F. Xue, W.-J. Hu, L.-J. Li, *NPJ 2D Mater Appl.*, **2018**, *2*, 18.

[23] A. L. Friedman, A. T. Hanbicki, F. K. Perkins, G. G. Jernigan, J. C. Culbertson, P. M. Campbell, *Sci. Rep.*, **2017**, *7*, 3836.

[24] M. Calandra, *Phys. Rev. B*, **2013**, *88*, 245428.

[25] S. N. Shirodkar, U. V. Waghmare, *Phys. Rev. Lett.*, **2014**, *112*, 157601.

[26] P. A. Thomas, G. H. Auton, D. Kundys, A. N. Grigorenko, V. G. Kravets, *Sci. Rep.*, **2017**, 7, 45196.

[27] S. Jiménez Sandoval, D. Yang, R. F. Frindt, J. C. Irwin, *Phys. Rev. B*, **1991**, *44*, 3955.

[28] Y. Yu, G.-H. Nam, Q. He, X.-J. Wu, K. Zhang, Z. Yang, J. Chen, Q. Ma, M. Zhao, Z. Liu, F.-R. Ran, X. Wang, H. Li, X. Huang, B. Li, Q. Xiong, Q. Zhang, Z. Liu, L. Gu, Y. Du, W. Huang, H. Zhang, *Nat. Chem.*, **2018**, *10*, 638.

[29] D. A. B. Miller, D. S. Chemla, S. Schmitt-Rink, *Phys. Rev. B*, **1986**, *33*, 6976.

[30] F. Fernández, K. Hegnerová, M. Piliarik, F. Sanchez-Baeza, J. Homola, M P. Marco, *Biosens. Bioelectron*., **2010**, *26*, 1231.

[31] J. Yuan, J. Addo, M.-I. Aguilar, Y. Wu, *Anal. Biochem.*, **2009**, *390*, 97.

[32] L. Zhou, N. Gan, Y. Zhou, T. Li, Y. Cao, Y. Chen, *Talanta*, **2017**, 167, 544.

[33] X. Yu, Y. He, J. Jiang, H. A. Cui, *Anal. Chim. Acta*, **2014**, *812*, 236.

[34] S. Zhang, Z. Zhang, W. Shi, S. A. Eremin, J. Shen, *J Agric. Food Chem*., **2006**, *54*, 5718.

[35] C. I. L. Justino, A. C. Duarte, T. A. P. Rocha-Santos, *Trends Analyt. Chem*., **2016**, *85*, 36.

[36] M. Thevis, A. Thomas, W. Schänzer, *Expert Rev. Proteomics*, **2014**, *11*, 663.

[37] F. Long, A. Zhu, H. Shi, *Sensors*, **2013**, *13*, 13928.

[38] B. Brehm-Stecher, C. Young, L.-A. Jaykus, M. L. Tortorello, *J. Food Prot*., **2009**, *72*, 1774.

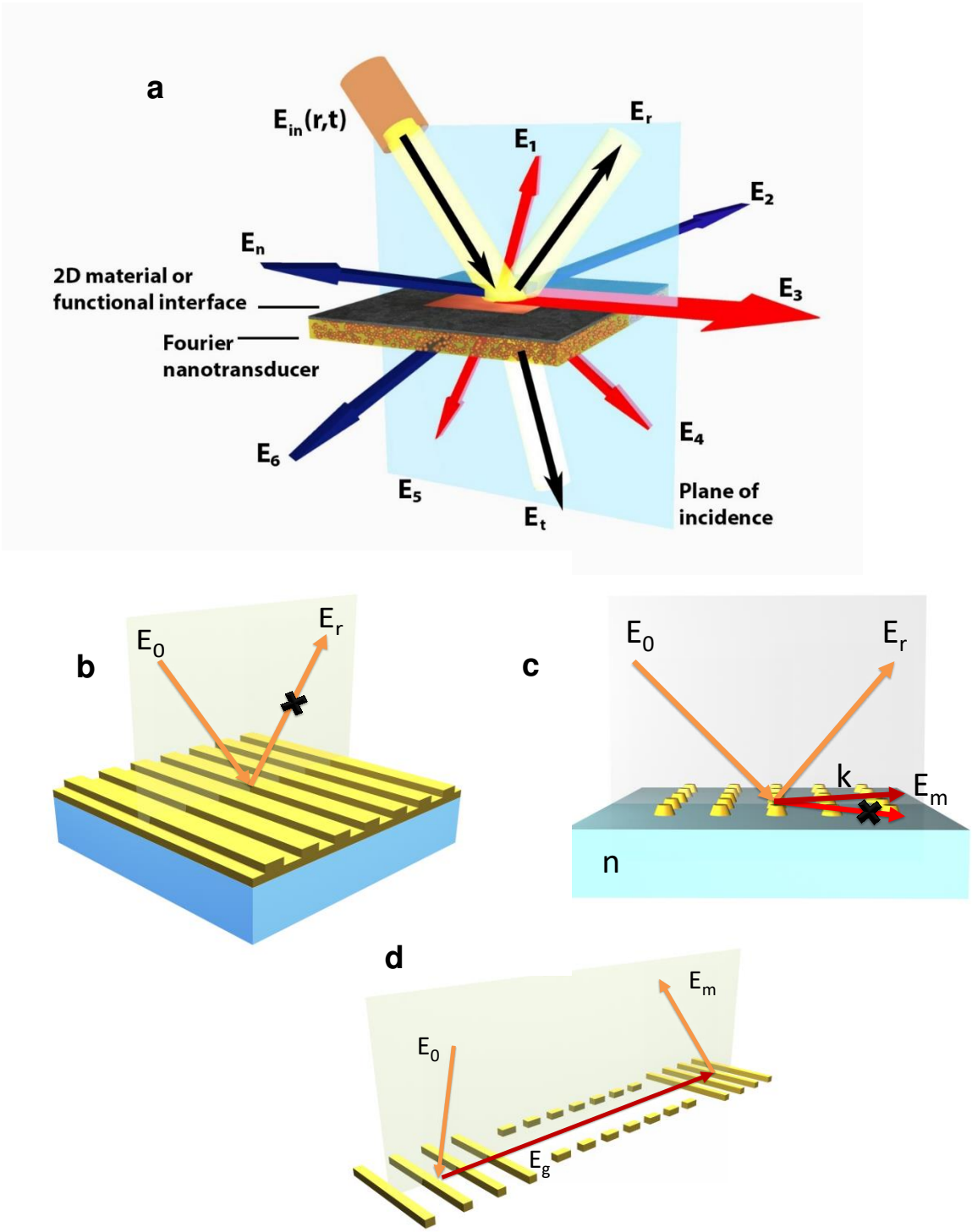

Figure 1. Phase Fourier nanotransducers (PFNs): a) General concept. Light beam is directed onto a transducer, which is capable of concentrating light in a tested 2D object, while optical information on the event is encoded in just a few coherent beams: reflected and transmitted (black arrows), diffracted in the plane of incidence (red arrows) and out of this plane (blue arrows); b) PFNs enabling a drastic drop of intensity in reflected, transmitted or diffracted beams due to absorption in the system or other phenomena; c) PFNs enabling the disappearance of a diffraction order (Rayleigh cut-off) or a redistribution of energy between them; d) PFNs enabling light coupling to a guiding mode along nanomaterial elements

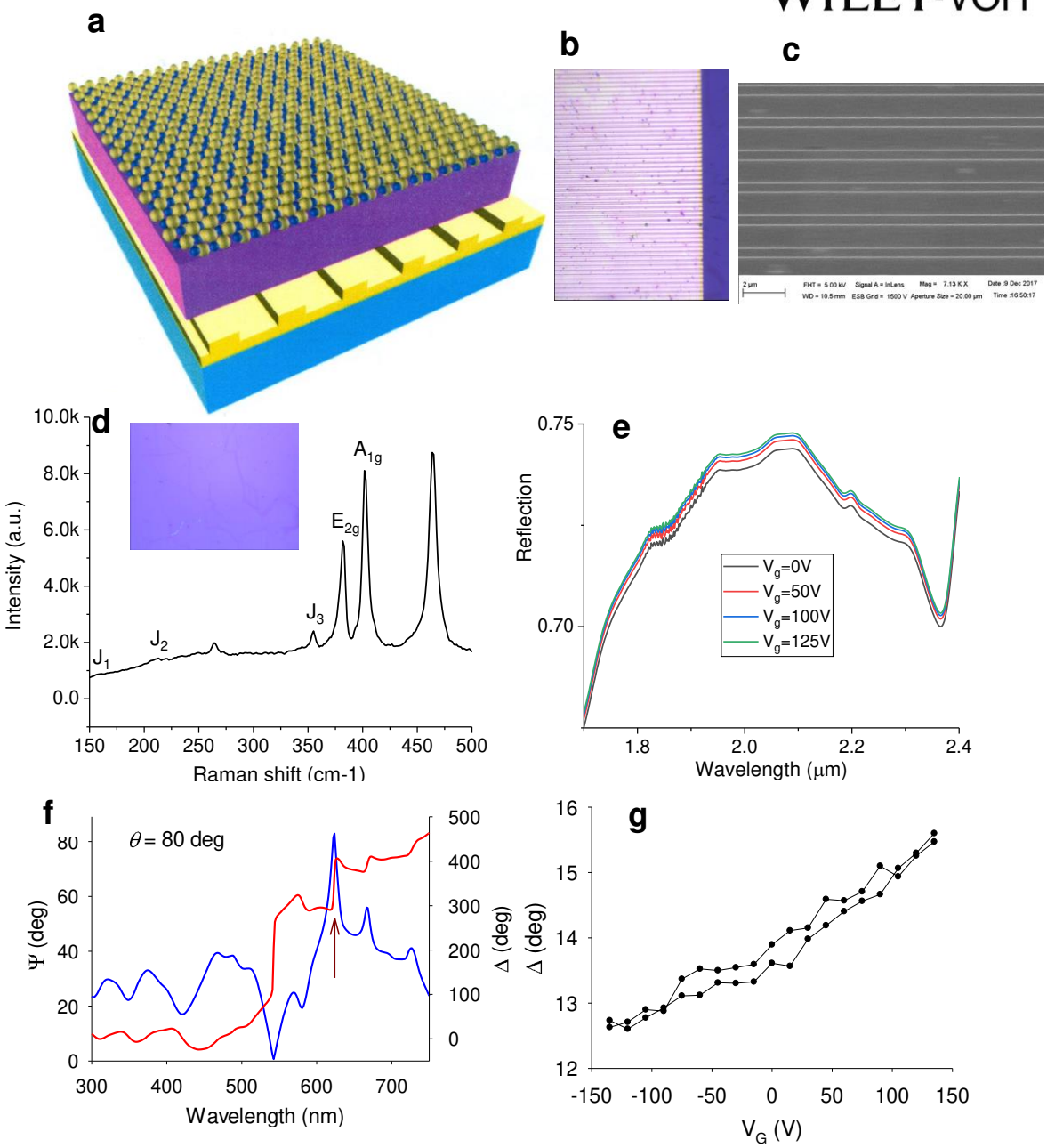

Figure 2. PFNs for study of ferroelectric response from a single atomic layer of MoS_2. a) Schematics of the structure used for studying ferroelectricity in MoS_2. The PFNs structure comprises glass substrate, 65 nm gold film, gold grating, 300 nm Si_3N_4 waveguide which also serves as a dielectric separator, a single layer CVD MoS_2 flake. The gating voltage is applied between the gold layer and the MoS_2 flake. b) The optical image of the structure. c) The SEM image of the structure. d) The Raman spectrum of MoS_2 flake from the region with presence of 1T phase. J_1, J_2 and J_3 mark Raman peaks corresponding to 1T' phase of MoS_2. E_{2g} and A_{1g} indicate peaks corresponding to 1H phase of MoS_2. The inset shows the optical image of the region from which spectra were acquired. e) The change of the sample reflection measured at normal angle of incidence due to applied gating voltage. f) A typical ellipsometric spectrum measured from the full structure at an incident angle of 80°. The blue line represents the amplitude response Ψ, the red line – phase response Δ. The dark red arrow indicates the point of vanishing reflection of *s*-polarization, $r_s \to 0$. g) The phase response of PFNs combined with MoS_2 at the wavelength of 630 nm as a function of gating voltage.

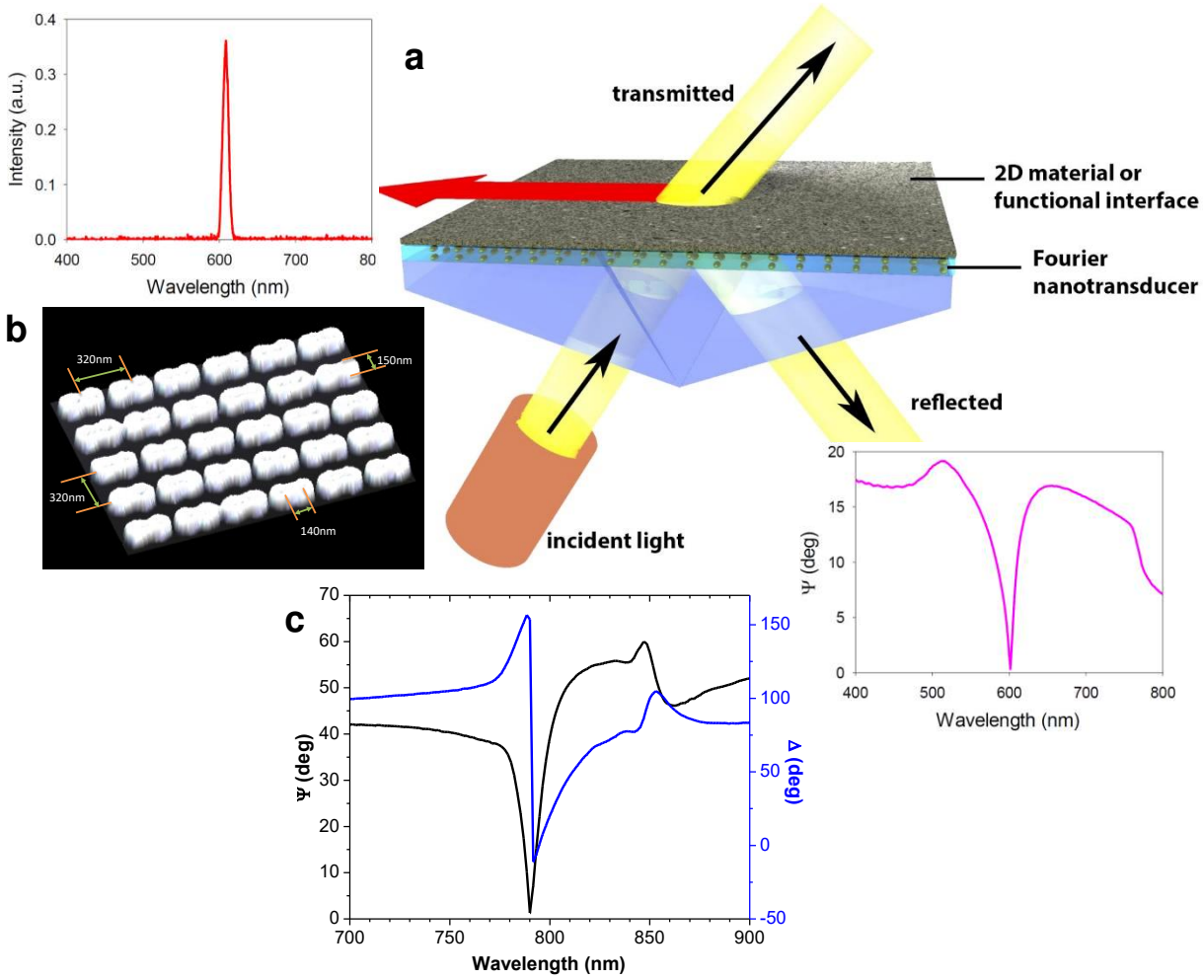

Figure 3. Diffraction edge phenomenon in PFNs based on 2D plasmonic nanoarray. a) Schematics of experiment for probing properties of functional interfaces using ellipsometry platform in ATR geometry. PFN is arranged in such a way that one of diffracted orders propagates over nanostructured transducer and is confined in 2D plane of the tested object. As a result, one can observe a peak in the grazing beam spectrum (left inset) and a dip in the reflection spectrum (bottom inset). Any dynamic change of 2D material or interface can be recorded in reflected, transmitted and diffracted beams by following amplitude and phase characteriatics of light; b) Scanning Electron Microscopy image of 2D plasmonic array based on merged 150 nm nanoparticles used in our tests; c) Spectral dependencies of ellipsometric reflectivity Ψ (black) and phase Δ (blue) for light reflected from PFN array depicted in the panel b contacting with aqueous ambience in ATR geometry

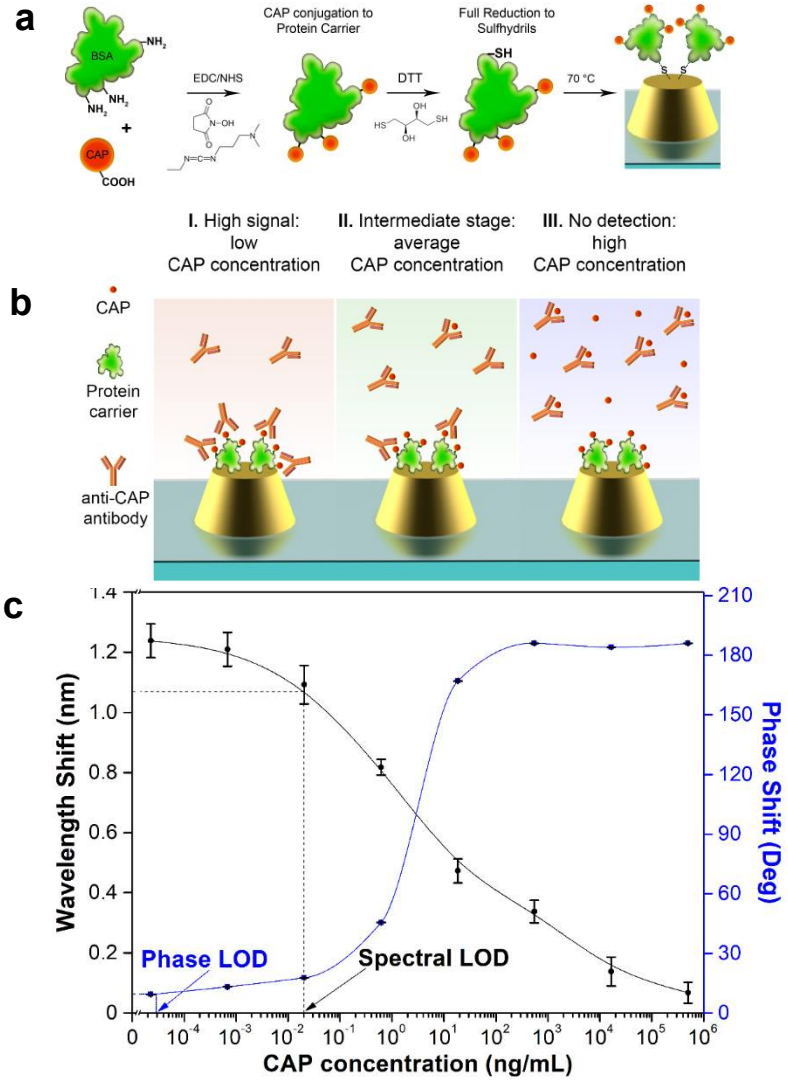

Figure 4. PFN in biosensing for study of antibiotic chloramphenicol (CAP) detection a) Functionalization of nanoparticle surface for enabling a protocol of chloramphenicol (CAP) detection. A carrier protein (bovine serum albumin, BSA) is first conjugated with CAP. BSA-CAP complex is then incubated with 1,4-Dithiothreitol (DTT) in carbonate-bicarbonate buffer. Then, DTT-treated BSA-CAP complex is immobilized on gold nanoparticles; b) In the competitive mode, CAP analyte in a sample under investigation is pre-incubated with anti-CAP antibody and the incubated complex (CAP*anti-CAP IgG) is pumped near CAP-coated Au nanoparticles. When CAP concentration is high, all antibodies are pre-blocked with CAP and their binding to surface-coated CAP is impossible (right panel). The decrease of CAP concentration leads to the appearance of free antibodies, which start to bind to CAP on the surface and the resulting signal is proportional to the number of surface-bound antibodies (middle panel). At low CAP concentrations (left panel) the recorded signal finally comes to a saturation corresponding to a complete binding of all sites on the surface of nanoparticles with antibodies (left panel); c) Dependence of spectral resonance minimum position (black) and light phase signal (blue) on concentration of CAP. The errors for spectral dependence were determined from the spectral resolution of the spectrometer ($\delta\lambda \cong 0.5$ nm) improved by fitting with the use of $N=7$ points to an experimental error of $\delta\lambda/\sqrt{N} \cong 0.2$ nm. The error was phase measurements was determined similarly and was about 0.05 Deg.